

See discussions, stats, and author profiles for this publication at: <https://www.researchgate.net/publication/252841644>

Radial speckle interferometry combined with a microindentation test to analyze coating adhesion

ARTICLE *in* PROCEEDINGS OF SPIE - THE INTERNATIONAL SOCIETY FOR OPTICAL ENGINEERING · SEPTEMBER 2010

Impact Factor: 0.2 · DOI: 10.1117/12.867643

CITATION

1

READS

22

4 AUTHORS, INCLUDING:



[Lucas P. Tendela](#)

National Scientific and Technical Research C...

6 PUBLICATIONS 13 CITATIONS

[SEE PROFILE](#)



[Matias R. Viotti](#)

Federal University of Santa Catarina

48 PUBLICATIONS 178 CITATIONS

[SEE PROFILE](#)



[Guillermo H Kaufmann](#)

Instituto de Física Rosario

172 PUBLICATIONS 1,733 CITATIONS

[SEE PROFILE](#)

RADIAL SPECKLE INTERFEROMETRY COMBINED WITH A MICROINDENTATION TEST TO ANALYZE COATING ADHESION

L. P. Tendela^a, M. R. Viotti^b, A. Albertazzi^b and G. H. Kaufmann^a

^aInstituto de Física Rosario (CONICET - UNR), S2000EZP Rosario, Argentina

^bLaboratório de Metrologia e Automatização, Universidade Federal de Santa Catarina
CEP 88040-970 Florianópolis, Brasil

ABSTRACT

This paper presents a novel technique to investigate coating adhesion using a radial speckle interferometer and a microindentation test. The proposed technique is based on the measurement of the radial in-plane displacement field produced by a microindentation introduced on the coated surface of the specimen. The advantages and limitations of the proposed technique are shown.

Keywords: DSPI, radial in-plane interferometry, adhesion, indentation test, epoxy resin

1. INTRODUCTION

The application of a coating to a substrate offers engineers the opportunity to modify the surface properties of a component, independently of the bulk properties. The development of new production techniques has opened up the use of coatings in a wide range of different industries. In all these cases, a good adhesion of the coating to the substrate is needed. Among common coatings which are used in industry we can mention epoxy resins. The role of these coatings is very important because they control various mechanical properties and also the corrosion resistance of the component. Although the loads are carried by the substrate, the mechanical performance depends to a large extent on the resin modulus and the failure strain, and also on the adhesion of the resin to the substrate.

As the definition of adhesion is not a simple issue, the characterization of this property has also generated considerable debate in the technical literature [1]. Adhesive performance tests are usually expressed as a failure limit and it can be measured as the maximum applied tension to separate the coating from the substrate [2]. It is also possible to assess the factors which contribute to the adhesive performance. Such factors can include the presence of flaws and poor contact, the modulus of elasticity of the substrate and the coating, and the sensitivity to environmental factors such as the contamination with moisture. There are various test methods that can be used to evaluate the adhesion of a given substrate-coating combination. However, several of these tests are qualitative or semi-quantitative and the adhesion is assessed from the appearance of the fracture surface [3]. Therefore, it is clear that in order to fully exploit the advantages that coatings can offer, it is essential to have a suitable adhesion test method to guarantee the user expectations.

The indentation test is a simple semi-destructive technique to assess the adhesion of thin coatings to hard substrates, such as an epoxy resin glued to a steel component. In the indentation test, an indenter introduces a pressure over the coated substrate in the normal direction. The tensile stress developed just outside the contact area tends to separate the interface and if adhesion between the coat and substrate is inadequate, debonding occurs [1].

The local displacement field that is produced by an indentation on a coated surface can be measured accurately using digital speckle pattern interferometry (DSPI) [4]. This technique is very attractive to be applied in optical metrology, not only for its non contacting nature but also for its relative speed of inspection procedure, mainly due to the use of video detection and digital image processing. The application of digital techniques in DSPI allows the automation of the data

*tendela@ifir-conicet.gov.ar; phone 54 341 4853200 × 120; ifir-conicet.gov.ar

analysis process, which is usually based on the extraction of the optical phase distribution encoded by the generated correlation fringes. Quite recently, Dolinko et al. [5] presented a method which combines DSPI with a bending test to evaluate coating adhesion and they also demonstrated that the deflections measured with this technique can be used to estimate the dimension of an artificially introduced defect which simulated the delaminated region generated by the bending stress. Unfortunately, even though this method can be used to estimate the adhesion of a real substrate-coating interface, it is not a very practical approach as the application of the bending test needs specially prepared coated specimens. A more practical way of introducing a perturbation in a coating–substrate system is by using an indentation test.

In this paper, a novel method to investigate coating adhesion is proposed which combines a radial in-plane speckle interferometer and a microindentation test. It is worth to note that DSPI has been already applied to the measurement of the local displacement field generated by an indentation [6,7]. Using steel specimens coated with a thin coating of epoxy resin and subjected to different adhesive conditions, it will be demonstrated that DSPI can be used to measure the small local deflections generated by the buckling due to introduction of the microindentation.

2. PRINCIPLES OF RADIAL IN-PLANE SPECKLE INTERFEROMETER

This section describes the working principle of the radial in-plane speckle interferometer [8] used in this work. The most important element of the interferometer is an annular diffractive optical element (DOE) formed by a grating of binary circular lines with a radial pitch p_r . A central clear window is left for viewing proposes, as shown in Fig. 1(a). Figure 1(b) shows a cross section of the DOE used to bend the light rays toward the center of the circular region. This figure displays four particularly chosen light rays diffracted from a collimated illumination source. Only the first diffraction order is shown in the figure. If a point P is particularly considered, the diffracted rays illuminate it symmetrically along the illumination directions indicated by the unitary vectors \mathbf{k}_1 and \mathbf{k}_2 . The sensitivity direction is given by the vector \mathbf{k} obtained from the subtraction of the two unitary vectors. If the angle between the illumination directions and the DOE axis are the same for both light rays, in-plane sensitivity will be reached at point P along the radial direction.

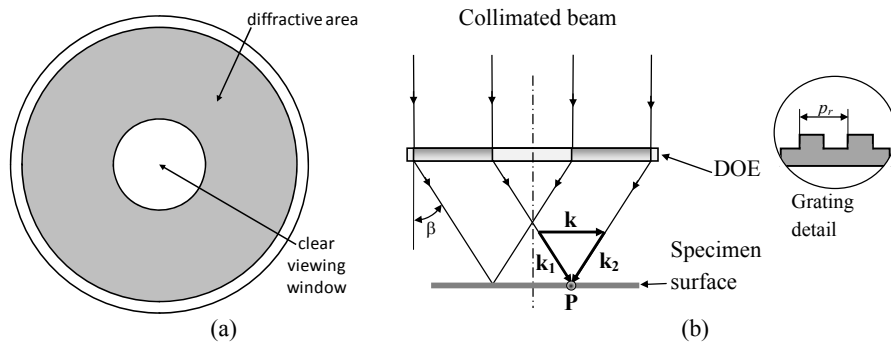


Figure 1. (a) Top view of the DOE. (b) Cross section of the diffractive optical element showing the principle of the radial in-plane sensitivity.

The description shown in Fig. 1 can be extended to any other cross sections of the diffractive element. Therefore, each point on the specimen surface will be illuminated by only one pair of light rays obtaining radial in-plane sensitivity for an illuminated circular region. The only exception is the central point of the circular area, which is a singular point. Radial in-plane sensitivity is very convenient for engineering applications to measure strains and stresses, and it only requires one illumination setup to acquire all valuable information.

It is well known that if the incident light is monochromatic, the grating will generate an array of angularly spaced beams with their directions given by [9]

$$\sin \xi = \frac{m\lambda}{p_r} \quad (1)$$

where ξ is the diffraction angle of the m -order, λ is the wavelength of the incident light and p_r is the period of the grating structure. It is worth to note that the diffraction angle is a function of the wavelength. The angle remains constant

only if the wavelength is constant. For a radial in-plane interferometer, as shown in Fig. 1, the radial component of the in-plane displacement field $u_r(r, \theta)$ can be computed from the measured optical phase distribution from [4]

$$u_r(r, \theta) = \frac{\phi(r, \theta)\lambda}{4\pi \sin \beta} \quad (2)$$

where $\phi(r, \theta)$ is the continuous phase distribution, and β is the angle between the direction of illumination and the normal to the specimen surface.

From Fig. 1, it is clear that the diffraction angle ξ and the angle β between the direction of illumination and the normal to the specimen surface have the same magnitude. Therefore, $\sin \xi = \sin \beta$. By replacing Eq. (1) in Eq. (2) and considering only the first-order diffraction $m = 1$, we have

$$u_r(r, \theta) = \frac{\phi(r, \theta)p_r}{4\pi} \quad (3)$$

According to Eq. (3), the relationship between the displacement field and the optical phase distribution depends on the period of the grating of the DOE and not on the laser wavelength. This particular effect can be understood taking into account that when the wavelength of the illumination source increases/decreases, the sine function of the diffraction angle decreases/increases in the same amount (see Eq. (1)). As in Eq. (2) λ is divided by $\sin \beta$, the ratio between them will also be constant. Therefore, the application of a diffractive optical element allows the use of non-wavelength stabilized diode lasers, which are compact, robust and less expensive.

3. EXPERIMENTAL PROCEDURE

3.1 Experimental setup

A diagram of the radial in-plane interferometer used to measure the radial in-plane displacement of the coating due to the introduction of the microindentation is shown in Fig. 2. The light beam of a diode laser L with a wavelength $\lambda = 0.658\mu m$ is expanded and then pass through the central hole of mirror M_1 , which forms an angle of 45° with the axis of the DEO. Mirrors M_2 and M_3 reflect back the laser beam to mirror M_1 being directed to the lens (CL) to obtain an annular collimated beam. Finally, the light is diffracted by the DOE, mainly in the first-order diffraction, towards the specimen surface. The residual zero-order diffracted light or light from higher order diffractions did not produce a troublesome situation since they did not impinge on the central measuring area over the specimen surface.

Mirror M_2 is linked to a piezoelectric actuator PZT which is used to introduce the phase shifts needed to evaluate the phase distribution. On the contrary, mirror M_3 is fixed and has a circular hole with a diameter slightly larger than the one located in M_2 . The PZT actuator linearly moves M_2 along its axial axis generating a relative phase difference between beams reflected by M_2 (the central beam) and M_3 (the external one). The dashed lines in Fig. 2 show boundaries between them. According to this figure, it is clear that for every couple of rays that reach every point laying on the specimen surface, one of them comes from M_2 and other from M_3 . Therefore, the PZT enables the introduction of a constant phase shift between both beams in order to calculate the wrapped phase map by using a phase shifting algorithm.

The intensity of the incident light is not constant over the whole circular area on the specimen surface, being particularly higher at the central point, because this singular point receives light contributions from all cross sections. In consequence, a very bright spot will be visible at the central part of the circular measurement region and consequently fringe quality will be reduced. For this reason, the outlier diameter (mirror M_2) as well as the hole diameter (mirror M_3) are computed to obtain a gap of approximately 1 mm, so that the light rays reflected to the center of the measurement area are blocked.

The angle between the directions of illumination and the normal to the specimen surface is chosen as 30° . The monitoring is made by an on-board CCD camera Point Gray FL2-20S4M/C, which output is digitized with an imaging card located inside the portable computer, with a resolution of 1600×1200 pixels and 256 gray levels (8 bits). This camera provides a small field of view which includes an illuminated area of about 10mm in diameter over the sample.

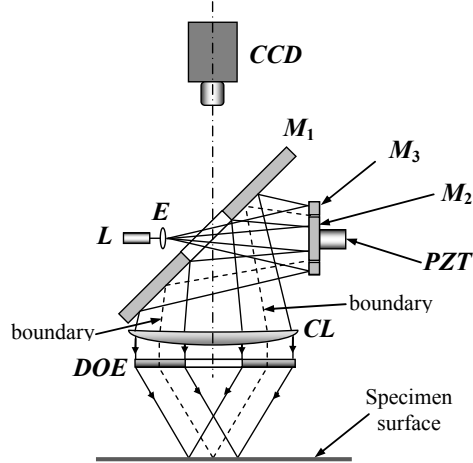


Figure 2. Optical arrangement of the radial in-plane speckle interferometer.

The microindentation was introduced using an indenter. This device has a Rockwell C spherical diamond tip of 0.2mm of radius and a cone angle of 120°, and a spherical tip of 2.5mm of diameter. The indenter was brought near to the specimen and then it was pressed into contact until the peak force was achieved. The indenter force was held constant during a certain time and afterwards the tip was withdrawn from the sample at a rate that was comparable to the loading rate until the force achieved the 10% of the peak value. Finally, the indenter was withdrawn from the specimen completely.

As substrate of the specimens we have used steel plates with a rectangular cross-section and a size of $50 \times 35 \times 5$ mm³. The epoxy resin used as the coating had a thickness of approximately 1mm. One of the main problems to investigate adhesion is the difficulty of preparing samples in which this property can be varied over a wide range. For this reason, different interface conditions were obtained by polishing the surface of the steel substrates with sandpapers of different grain sizes. In order to obtain reproducible interface conditions, the polishing was performed by displacing the sandpaper along the same direction in all samples. It is supposed that the different depths of the parallel microgrooves generated in the polished substrate surfaces will change the effective adhesion.

3.2 Data analysis

The procedure used to record the pair of speckle interferograms to be correlated was as follows. The speckle interferometer and the indenter were fixed to a special base by an interface that allowed a fast and accurate repositioning of the measurement and the loading modules. Each specimen was fixed with a holder specifically designed to avoid the introduction of rigid body displacements due to the generation of the microindentation. Afterwards, a set of phase-shifted speckle interferograms was acquired, and the reference phase distribution was computed and stored in the computer. Then, the measurement module was taken off and was replaced by the indenter. An indentation was introduced as explained above and a new set of phase-shifted speckle interferograms was acquired. Finally, the corresponding wrapped phase distribution was calculated and stored.

In the last step, the wrapped phase difference map was evaluated and the continuous phase distribution was obtained by applying a flood fill phase unwrapping algorithm [10]. Finally, the radial in-plane displacement field generated in the neighbourhood of the indentation was computed from the phase distribution by using Eq. (3).

4. EXPERIMENTAL RESULTS

In order to determine the performance of the DSPI and indentation combined system, the radial in-plane displacement component generated by the microindentation was first evaluated in specimens having different coating–substrate interface conditions. Figure 3 shows the wrapped phase map obtained with the conical indenter by testing two specimens with their substrates polished with different sandpapers.

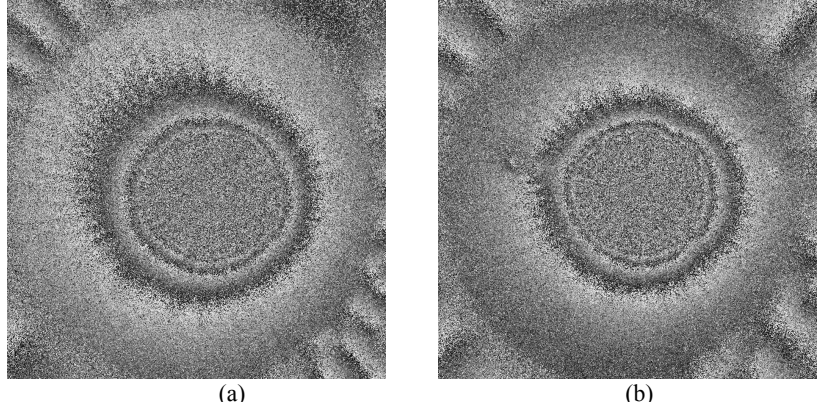


Figure 3. Wrapped phase maps produced by specimens with different interface conditions using the conical indenter for a peak force of 150N: (a) substrate polished with sandpaper number 80; (b) substrate polished with sandpaper number 600.

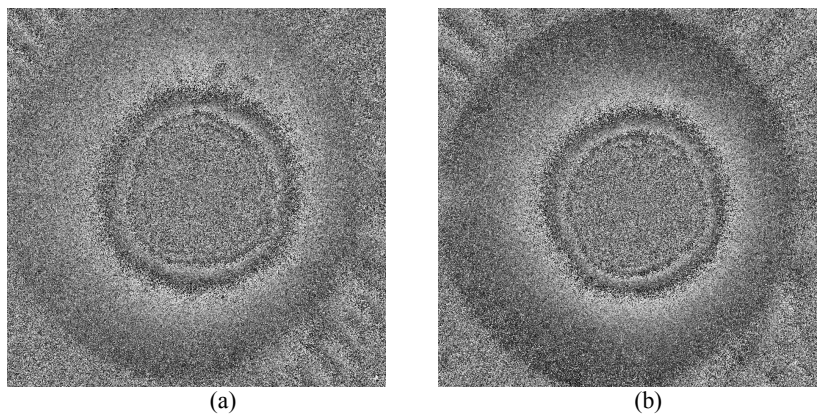


Figure 4. Wrapped phase maps produced by specimens with different interface conditions using the spherical indenter for a peak force of 150N: (a) substrate polished with sandpaper number 80; (b) substrate polished with sandpaper number 600.

Figure 4 displays the wrapped phase map obtained by testing the same substrates with the spherical indenters. In both cases, the peak force achieved was 150N. In Figs. 3 and 4, it is observed that the local wrapped phase maps have a circular shape. Therefore, these local wrapped phase distributions confirm that the displacement field introduced by the microindentation was axisymmetrical, as expected. Furthermore, these figures also show that the displacement field produced by a microindentation introduced on the coated surface of the substrate increases when the grain size of the sand paper was reduced (see Fig. 5).

As can be seen in Figs. 3, 4 and 5, the radii of the regions that present speckle decorrelation produced do not depend on the adhesion of the coating to the substrate. They only depend on the mechanical properties and the load used to introduce the microindentation, as shown in Fig. 6.

The local displacement component was also measured for different values of the indentation load. As expected, the results displayed in Fig. 6 show that as the applied force increases, the radii of the regions presenting speckle decorrelation increases as well. The microindentations were introduced in a single specimen in order to make sure that the same interface conditions were used in all tests. As mentioned before, the radial in-plane displacement component produced by a microindentation along a radial direction presents significant difference when specimens with different interface conditions were tested. Figures 7 and 8 show the indentation marks left on the coated surface of the specimen displayed in Fig. 6, where the radii of these marks are smaller than the radii of the region presenting speckle decorrelation.

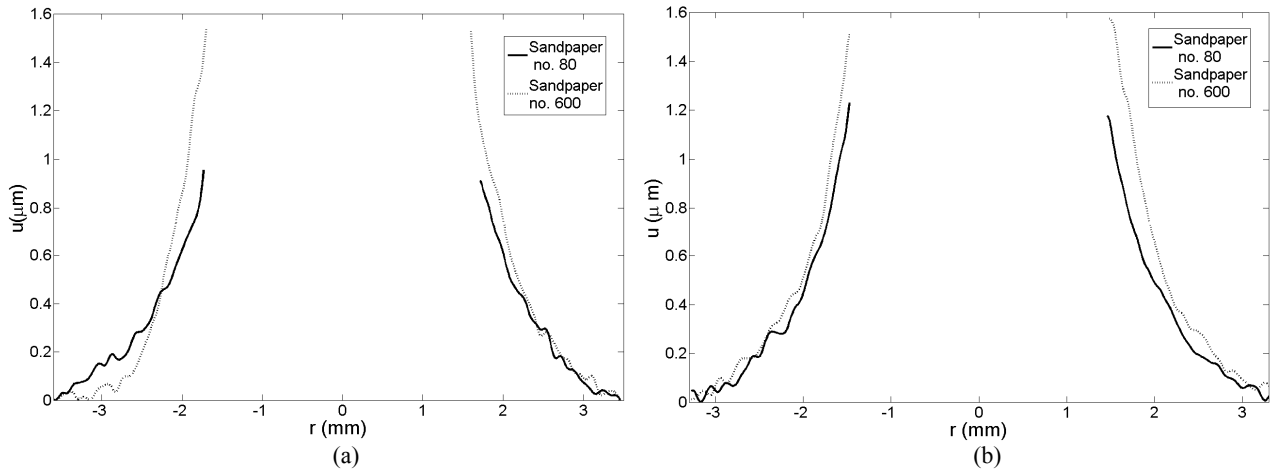


Figure 5. Radial in-plane displacement component produced by a microindentation along a radial direction for specimens with different interface conditions and a peak force of 150N using: (a) the conical indenter; (b) the spherical indenter.

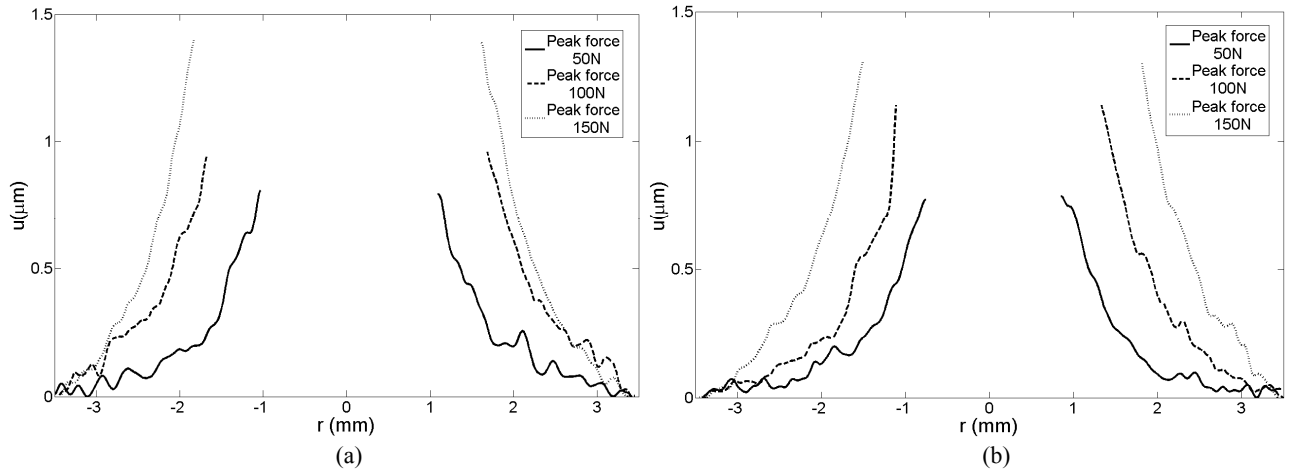


Figure 6. Radial in-plane displacement component produced by a microindentation on the coated surface of the specimen polished with sandpaper number 320 for different peak loads using: (a) the conical indenter; (b) the spherical indenter.

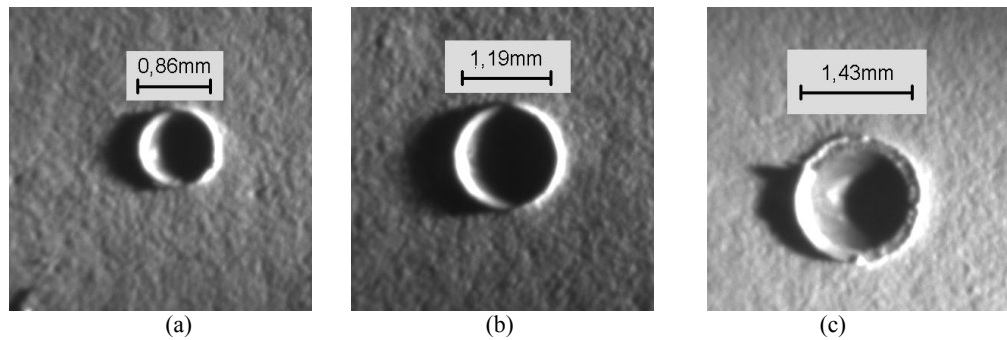


Figure 7. Marks of the conical indenter left on the coated surface of the specimen polished with sandpaper number 320 for a peak load of: (a) 50N; (b) 100N; (c) 150N.

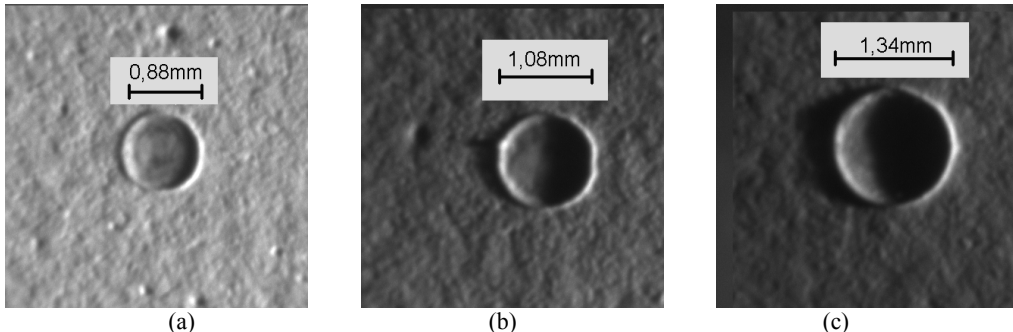


Figure. 8. Marks of the spherical indenter left on the coated surface of the specimen polished with sandpaper number 320 for a peak load of: (a) 50N; (b) 100N; (c) 150N.

5. CONCLUSIONS

This paper presents an evaluation of a technique based on a radial speckle interferometer and a microindentation test, which is proposed to investigate coating adhesion. The experiments performed on coated specimens with different interface conditions demonstrate that DSPI can be used to assess the adhesion of the coating to the substrate. These data allow the determination of the radius of fringes produced by a microindentation introduced on the coated surface, which is directly relevant for the estimation of the adhesion strength.

The localized plastic deformation generated by the indentation process produces a permanent displacement field around it, which is a function of the shape of the indenter, the applied load and the mechanical properties of the material. Using the continuous phase distribution obtained from the measurements allow the determination of the local radial in-plane displacement field which can be used to assess the coating adhesion.

The obtained results demonstrate that the proposed technique could be used as a valuable tool to investigate the adhesion performance of coatings. Furthermore, as the size of the microindentation needed for the measurements is very small, the method can be considered as nearly non destructive. Therefore, a portable speckle interferometer combined with a microindentation device result a quite adequate system to be used in industry for in-line testing of different coated components.

Additional investigations are necessary to develop a practical approach which can be used to quantify coating adhesion. This work will involve the development of an appropriate model to calculate the adhesion strength from the measurement of the displacement field using inverse analysis and a fracture mechanics approach. These investigations will be the object of future work.

REFERENCES

- [1] Lacombe, R., [Adhesion measurement methods], Taylor & Francis, Boca Raton, 1-69 (2006.).
- [2] Graystone, J. and Kennedy, R., "Prospects for assessing the adhesive performance of coatings by non-destructive methods," *Surface Coatings International Part B: Coatings Transactions*, 88(3), 163-178 (2005).
- [3] Ollendorf, H. and Schneider, D., "A comparative study of adhesion test methods for hard coatings," *Surface and Coatings Technology*, 113(1-2), 86-102 (1999).
- [4] Rastogi, P. K., [Digital Speckle Pattern Interferometry and Related Techniques], Wiley, Chichester, 142-224 (2001).
- [5] Dolinko, A. E. and Kaufmann, G. H., "Feasibility study of a digital speckle pattern interferometry and bending test combined technique to investigate coating adhesion," *Opt Lasers Eng*; 46(3), 230-235 (2006).
- [6] Dolinko, A. E. and Kaufmann, G. H., "Measurement of the local displacement field generated by a microindentation using digital speckle pattern interferometry and its application to investigate coating adhesion," *Optics and Lasers in Engineering*, 47(5), 527-531 (2009).

- [7] Viotti, M. R., Kaufmann, G. H. and Galizzi, G. E., "Measurement of elastic moduli using spherical indentation and digital speckle pattern interferometry with automated data processing," *Optics and Lasers in Engineering*, 44(6), 495–508 (2006).
- [8] Viotti, M. R., Kapp, W. A. and Albertazzi, Jr. A., "Achromatic digital speckle pattern interferometer with constant radial in-plane sensitivity by using a diffractive optical element," *Applied Optics*, 48(12), 2275-2281 (2009).
- [9] Hetch, E. and Zajac, A., [Optics], Addison-Wesley Publishing Company, San Fransisco, 443-514 (2002).
- [10] Asundi, A. and Wenzen, Z., "Fast phase-unwrapping algorithm based on a gray-scale mask and flood fill," *Applied Optics*, 37(23), 5416-5420 (1998).